

Nanomechanical Properties of Thin Films of Type I Collagen Fibrils

Koo-Hyun Chung,^{*,†} Kiran Bhadriraju,[‡] Tighe A. Spurlin,[‡] Robert F. Cook,[†] and Anne L. Plant[‡][†]Materials Science and Engineering Laboratory, National Institute of Standards and Technology, Gaithersburg, Maryland 20899 and [‡]Chemical Science and Technology Laboratory, National Institute of Standards and Technology, Gaithersburg, Maryland 20899

Received August 17, 2009. Revised Manuscript Received December 28, 2009

The mechanical cues that adherent cells derive from the extracellular matrix (ECM) can effect dramatic changes in cell migration, proliferation, differentiation, and apoptosis. Model ECMs composed of collagen fibrils formed from purified collagen are an important experimental system to study cell responses to mechanical properties of the ECM. Using a self-assembled model system of a film composed of 100–200 nm diameter collagen fibrils overlaying a bed of smaller fibrils, we have previously demonstrated changes in cellular response to systematically controlled changes in mechanical properties of the collagen. In this study, we describe an experimental and modeling approach to calculate the elastic modulus of individual collagen fibrils, and thereby the effective stiffness of the entire collagen thin film matrix, from atomic force microscopy force spectroscopy data. These results demonstrate an approach to the analysis of fundamental properties of thin, heterogeneous, and organic films and add further insights into the mechanical and topographical properties of collagen fibrils that are relevant to cell responses to the ECM.

Introduction

Collagens are a family of cell-adhesive proteins that are a major constituent of the extracellular matrix (ECM).¹ Cells interact with ECM proteins such as collagen primarily through integrin receptors, and the ligation of specific integrins in part determines cell response to the local physiological environment by initiating intracellular signaling events. In addition to the role of ECM receptor ligation, many studies have also shown that the mechanical properties of the ECM can have a great influence on cell responses such as migration, proliferation and differentiation.^{2–6}

Thin films of Type I collagen have allowed us to examine the effects of changes in mechanical properties of collagen on cell response without altering receptor engagement or collagen supramolecular structure.^{6,7} Films of collagen are formed by self-assembly of collagen at hydrophobic surfaces such as alkanethiol monolayers⁷ or untreated polystyrene.⁸ Collagen monomers adsorb at hydrophobic surfaces and at sufficiently high solution concentrations apparently nucleate the self-assembly of fibrils of 100 to 200 nm in diameter. These larger fibrils appear to grow out of, and sit on top of, a layer of smaller diameter (< 50 nm) fibrils. In addition, we have illustrated that collagen fibrils formed by the neutralization of acid-solubilized collagen monomers form fibrils that have a supramolecular structure and banding pattern

(Supporting Information, Figure S1) similar to those seen in collagen gels and *in vivo*.⁹ These structures are consistent with collagen structures that exist *in vivo* and with structures in collagen gels.¹

Studies with collagen films have strongly suggested that the mechanical properties of the larger collagen fibrils play a critical role in determining cell response.⁶ At an overall thickness of approximately 600 nm, films of collagen allow for clear microscopic observations of cells moving and reorganizing the larger collagen fibrils. Furthermore, cells on collagen films exhibit the same responses as cells on collagen gels with respect to integrin engagement, and measurements of cell spreading and proliferation rates, tenascin-C gene expression, and other indicators of cell signaling responses^{6,7,10} are unaltered. These quantitative data strongly suggest that the mechanical signals provided by collagen gels are generated in a fibrillar matrix that provides mechanical signals from nano- and microscale structures similar to those occurring in the ECM.

There are many examples of altering, and measuring, bulk properties of cell culture materials, and relating material properties such as elastic modulus to particular cell responses.^{2,11} Such material properties are considerably more difficult to measure at the nano- and microscale, particularly under physiological aqueous conditions. Yet it is likely that responses to materials at these very small scales are highly relevant to cell biology, as they are on the scale of cellular structures such as focal adhesions. In this report, we present atomic force microscopy (AFM) measurements in imaging and force spectroscopy modes, together with a mathematical model, to estimate the elastic modulus of collagen films. The model considers the films as two-layer composites composed of an underlying bed of smaller fibrils covered with a layer

*Corresponding author. Telephone: (301) 975-5409. Fax: (301) 975-5334. E-mail: khchung@nist.gov.

(1) Nimni, M. E. In *Collagen*, Vol. 1: *Biochemistry*; Nimni, M. E., Ed.; CRC Press Inc.: Boca Raton, FL, 1988; pp 3–33.

(2) Pelham, R. J.; Wang, Y. L. *Proc. Natl. Acad. Sci. U.S.A.* **1997**, *94*, 13661–13665.

(3) Lo, C. M.; Wang, H. B.; Dembo, M.; Wang, Y. L. *Biophys. J.* **2000**, *79*, 144–152.

(4) Discher, D. E.; Janmey, P.; Wang, Y. L. *Science* **2005**, *310*(5751), 1139–1143.

(5) Engler, A. J.; Sen, S.; Sweeney, H. L.; Discher, D. E. *Cell* **2006**, *126*, 677–689.

(6) McDaniel, D. P.; Shaw, G. A.; Elliott, J. T.; Bhadriraju, K.; Meuse, C.; Chung, K. H.; Plant, A. L. *Biophys. J.* **2007**, *92*, 1759–1769.

(7) Elliott, J. T.; Tona, A.; Woodward, J. T.; Jones, P. L.; Plant, A. L. *Langmuir* **2003**, *19*, 1506–1514.

(8) Elliott, J. T.; Halter, M.; Plant, A. L.; Woodward, J. T. *Biointerphases* **2008**, *3*, 19–28.

(9) Kadler, K. E.; Holmes, D. F.; Trotter, J. A.; Chapman, J. A. *Biochem. J.* **1996**, *316*, 1–11.

(10) Langenbach, K. J.; T Elliott, J.; Tona, A.; McDaniel, D.; Plant, A. L. *BMC Biotechnol.* **2006**, *6*.

(11) Yeung, T.; Georges, P. C.; Flanagan, L. A.; Marg, B.; Ortiz, M.; Funaki, M.; Zahir, N.; Ming, W.; Weaver, V.; Janmey, P. A. *Cell Motil. Cytoskeleton* **2005**, *60*, 24–34.

of larger fibrils. The properties of both layers were determined independently from AFM force spectroscopy measurements using a sharp probe, and the predicted properties of the composite structure were validated by direct measurement using a colloidal probe. The report examines the nanoscale mechanical properties of collagen that might be sensed by cells and affect cellular response to the ECM.

Materials and Methods¹²

Preparation of Collagen Thin Films. Thin films of Type I collagen were prepared on alkanethiol treated gold coverslips from an acid stabilized monomer stock solution (Purecol, Nutacon BV, Leimuiden, Netherlands) as described previously.^{6,7} The fibrils were formed by noncovalent association of collagen monomers at neutral pH and were not additionally cross-linked in any way. Our protocol was to briefly expose the films to a stream of N₂ to cause the fibrils to collapse onto the surface in a reproducible manner. Collagen samples prepared in this way consist of small fibrils that grow on the surface of the coverslip and allow the polymerization of large fibrils to occur (Figure 1).^{7,13–15} Samples were kept under phosphate buffered saline (PBS) solution and stored at 4 °C until use. Hydrated samples were warmed to ambient temperature and examined with AFM under PBS. To generate a dehydrated condition, samples were dehydrated by removing the PBS, rinsed with H₂O, and then air-dried for 24 h on the AFM stage. The dehydrated samples were then recovered with PBS for an additional 24 h before AFM measurements. The coverslips had six square scratch marks (40 μm × 40 μm) inscribed on them using a diamond indentation probe, so the same sample regions could be located through the use of an inverted microscope before and after dehydration.

AFM Topographical Imaging. All AFM experiments were conducted at the NIST Advanced Measurement Laboratory in which the temperature was set at 20 °C and controlled within 0.02 °C. To reduce thermal drift, samples were allowed to equilibrate at room temperature for 24 h before collecting data at each condition tested. An MFP-3D AFM (Asylum Research, Santa Barbara, CA) attached to an inverted optical microscope was used to collect images in intermittent contact mode at a linear scan rate of 0.1–0.3 Hz using silicon nitride cantilever probes (Biolever, Olympus, Tokyo) with spring constants ranging from 0.023 to 0.026 N m⁻¹. The shape of the tip was directly determined by scanning electron microscopy. The probe tips were paraboloids of revolution, with cross-sectional radii, ρ , given by $\rho^2 = 4kh_c$, where h_c is the contact depth of the tip measured from the apex and k is the parabolic constant. For the tips used here, k was approximately 3 nm, leading to tip radii of approximately 20 nm. From AFM images, the surface roughness and the height of the large fibrils were determined at the same locations before and after dehydration. The surface roughness of the regions with small fibrils was also calculated by segmenting the regions corresponding to the large fibrils and removing their contribution from each image.

AFM Force Spectroscopy Measurements on Individual Collagen Fibrils and Fibril Bed. From AFM images of the collagen films collected using the references markings described above, force spectroscopy measurements were performed before and after dehydration using the probes used for imaging. Such measurements provide the force exerted by the probe tip on the

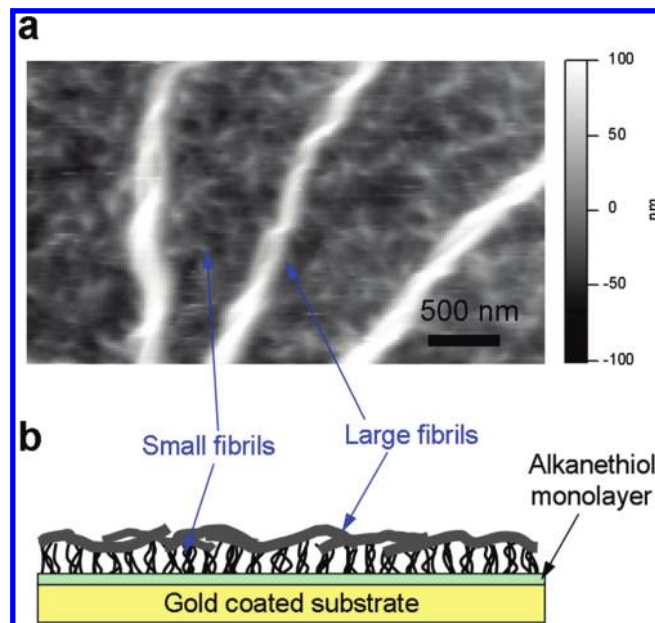


Figure 1. (a) AFM image that indicates both large collagen fibrils and a bed of small collagen fibrils are present in the samples. (b) Schematic diagram illustrating the structure of the collagen thin film. In previous studies performed by our laboratory^{7,13} and others,^{14,15} the large collagen fibrils were observed to grow out of the small bed of fibrils.

sample as a function of the imposed displacement of the cantilever. For indentation contact experiments, such as conducted here, the force, P , and penetration, h , of the tip into the sample surface are taken as positive when directed into the sample. The force–displacement data were converted into force–penetration data by subtracting the cantilever deflection from the displacement. Force–penetration data were obtained for both the individual larger collagen fibrils (100 to 200 nm diameter) and on the underlying bed of smaller fibrils (< 50 nm diameter) attached to the substrate (Figure 1).

To obtain an average value of the modulus for the bed of small fibrils, 40 force–penetration curves were collected at different locations on the bed of small fibrils before and after dehydration. The indentation modulus, E_S^* , of the bed of small fibrils was determined by fitting the curves to the relation appropriate to indentation by a parabolic probe:¹⁶

$$P = \frac{4}{3}E_S^*(2k)^{1/2}h^{3/2} \quad (1)$$

For an isotropic material (as assumed here), the indentation modulus is given by $E_S^* = E_S/(1 - \nu_S^2)$, where E_S and ν_S are the elastic modulus and Poisson's ratio, respectively, of the bed of small fibrils.

To ensure the force–penetration data were collected from the center of an individual large fibril, force–penetration data were first obtained across the fibril using a small normal peak force (0.5 nN) and the position with the least hysteresis chosen as the fibril center (Supporting Information, Figure S2). Between 10 and 20 force–penetration measurements to various peak forces ranging from 0.1 nN to 2 nN were performed for the large fibrils using an imposed probe displacement rate of 0.5 μm s⁻¹. Before each experimental trial, probe deflection sensitivities were calibrated on glass substrates and probe cantilever spring constants were determined using the thermal method.¹⁷ The longitudinal elastic modulus, E_L , of the long fibrils was determined by fitting the force–penetration measurements to a relation appropriate to a

(12) Commercial equipment and materials are identified in order to adequately specify certain procedures. In no case does such identification imply recommendation or endorsement by the National Institute of Standards and Technology (NIST), nor does it imply that the materials or equipment identified are necessarily the best available for the purpose.

(13) Elliott, J. T.; Woodward, J. T.; Umarji, A.; Mei, Y.; Tona, A. *Biomaterials* **2007**, *28*, 576–585.

(14) Pamula, E.; De Cupere, V.; Dufrene, Y. F.; Rouxhet, P. G. *J. Colloid Interface Sci.* **2004**, *271*, 80–91.

(15) Gurdak, E.; Dupont-Gillain, C. C.; Booth, J.; Roberts, C. J.; Rouxhet, P. G. *Langmuir* **2005**, *21*, 10684–10692.

(16) Sneddon, I. N. *Int. J. Eng. Sci.* **1965**, *3*, 47–57.

(17) Hutter, J. L.; Bechhoefer, J. *Rev. Sci. Instrum.* **1993**, *64*, 1868–1873.

stiff cylindrical beam on a compliant elastic foundation¹⁸ (see Supporting Information):

$$P = 4.30E_L^{1/4}k_0^{3/4}R^{1/4} \left[2 \left(\frac{h}{R} \right)^3 - \left(\frac{h}{R} \right)^4 \right]^{1/2} \quad (2)$$

where R is the radius of the large fibril and k_0 is the foundation modulus of the bed of small fibrils, given by

$$k_0 = \frac{(1 - \nu_S)E_S}{(1 + \nu_S)(1 - 2\nu_S)H} = \frac{E_S^*(1 - \nu_S)^2}{(1 - 2\nu_S)H} \quad (3)$$

and H is the foundation thickness. The thickness of the bed of small fibrils was estimated by force spectroscopy from the penetration at which indentation substrate effects were evident as significant contact stiffening. This thickness is a lower bound due to the possible presence of compressed small fibrils between the probe and substrate even at large forces.

AFM Force Spectroscopy Measurements on Collagen Thin Films. Colloidal probe force–penetration data were collected on the thin films before and after dehydration to obtain mechanical information averaged over a larger probe area. The experiments were performed over a peak force range of 5 nN to 300 nN at an imposed probe displacement rate of $0.5 \mu\text{m s}^{-1}$ using 30 μm diameter gold coated silicon colloidal probes (Novascan, Ames, IA) with normal spring constant of 1.29 N m^{-1} . About 20 force–penetration curves were obtained on ten randomly selected regions to determine average collagen thin film modulus values. Colloidal probe deflection sensitivities and spring constants were determined as stated above for the AFM probes.

Statistical Analyses. All experimental measurements are reported as mean \pm standard deviation. Effects of dehydration on film topography, dimensions, and properties were determined by paired or unpaired Student's t -tests at a significance level of $p = 0.05$.

Results

All data presented are the results of measurements performed on collagen films submersed in aqueous solution. To enable evaluation and interpretation of AFM data on collagen films, we measured films that were kept fully hydrated at all times, and films that were allowed to dehydrate for 24 h prior to being submersed in aqueous solution and measured. We have previously shown that collagen films that are allowed to dehydrate in air for more than a few hours provide a mechanically stiffened environment to cells, even after having been replaced in aqueous medium for periods of days.⁶ Cells are observed to physically manipulate collagen fibrils but can no longer do so if the films have been dehydrated. Cells on dehydrated films become well-spread and proliferative as is consistent with their response to a stiff matrix, and nanoindentation measurements of dehydrated large fibrils reveal increases in their contact stiffness.⁶ By comparing the properties of fully hydrated and dehydrated collagen films we hope to develop greater insight into the properties of collagen fibrils that are likely to be important to cell response.

Collagen Matrix Topography. As a first step in understanding the nanomechanical properties of collagen fibrils, AFM imaging was used to examine the nanoscale topography (Figure 2) with respect to the height of the fibrils and the roughness of the surface. These data are summarized in Table 1, and are used in subsequent models. For these analyses we chose areas in which extensive interactions between larger fibrils were

minimized. An example of such a region is shown in Figure 1. While these regions had less fibril coverage than most areas, the selection simplified the quantitative analysis of individual fibrils.

The centerline average roughness (R_a) from five ($5 \mu\text{m} \times 5 \mu\text{m}$) scans of fully hydrated collagen films was $R_a = 67 \pm 13 \text{ nm}$. Cross-sectional height profiles were also collected from 21 selected fibrils from five AFM images of fully hydrated fibrils as indicated in Figure 2a (area analyzed is indicated by $L-L'$). The mean height of the entire field was obtained by least-squares analysis, and was subtracted from the profiles. To obtain a better representation of the height of each large fibril, each height was determined by averaging 10 profiles taken across the fibril at different positions along its length. The average height of these isolated fibrils was $147 \pm 18 \text{ nm}$.

We also examined these same areas after allowing the films to dehydrate on the AFM stage. Dehydrated films showed significantly different topography. Previous reports have suggested an important role for water in fibril packing and mechanical stiffness.^{19,20} After dehydration, average roughness was observed to decrease to $R_a = 47 \pm 9 \text{ nm}$, and the average height of the large fibrils decreased to $118 \pm 15 \text{ nm}$. Despite the large standard deviations, when each area was compared before and after dehydration, a paired t -test indicated significant differences due to dehydration.

The role of the underlying bed of small fibrils in cell response has been unclear, largely because of its small dimensions. Parts d and e of Figure 2 show digitally magnified regions of the AFM images shown in Figure 2, parts a and b. The average roughness of the bed of small fibrils in fully hydrated samples was $45 \pm 12 \text{ nm}$. Significant decreases in roughness occurred in these areas in response to dehydration; roughness decreased to $30 \pm 7 \text{ nm}$. Topography of this layer also changed; profiles such as that shown in Figure 2f indicate the bed of the small collagen fibrils was substantially flattened on dehydration.

Elastic Modulus of Collagen Films. Knowing fundamental physical constants of collagen films, such as the elastic modulus, will enable us to understand the forces to which cells are responding, and to unambiguously compare data collected from cells on collagen films with data from cells on bulk protein or polymer matrices. We have addressed the challenges associated with determination of the physical mechanical constants of a very thin and heterogeneous material by treating it as a two-layered structure and analyzing each layer independently (Figure 1).⁶

Elastic Modulus of the Underlying Bed of Small Fibrils.

The reduced elastic modulus of the underlying bed of smaller fibrils, E_S^* , was determined from force–penetration curves, obtained in regions devoid of larger fibrils and analyzed using the Sneddon elastic contact model¹⁶ for a parabolic shaped probe. Figure 3a shows representative force–penetration curves obtained on the bed of smaller fibrils before and after dehydration to a peak force of 1.5 nN. As seen in Figure 3 the curves exhibit little hysteresis, suggesting a largely elastic response. In addition, the curves suggest that for forces greater than about 0.5 nN the probe begins to sample the underlying stiff gold-covered glass substrate. To minimize the effect of the stiff substrate on determination of the reduced elastic modulus, the model was fit to portions of the curves as depicted in the inset of Figure 3a.

The variation of E_S^* with penetration is shown in Figure 3b; the values of E_S^* are approximately constant up to penetrations

(19) Leikin, S.; Parsegian, V. A.; Yang, W. H.; Walrafen, G. E. *Proc. Natl. Acad. Sci. U.S.A.* **1997**, *94*, 11312–11317.

(20) Rosenblatt, J.; Devereux, B.; Wallace, D. G. *Biomaterials* **1994**, *15*, 985–995.

(18) Krenk, S., *Mechanics and Analysis of Beams, Columns, and Cables*, 2nd ed.; Springer: Berlin, 2001.

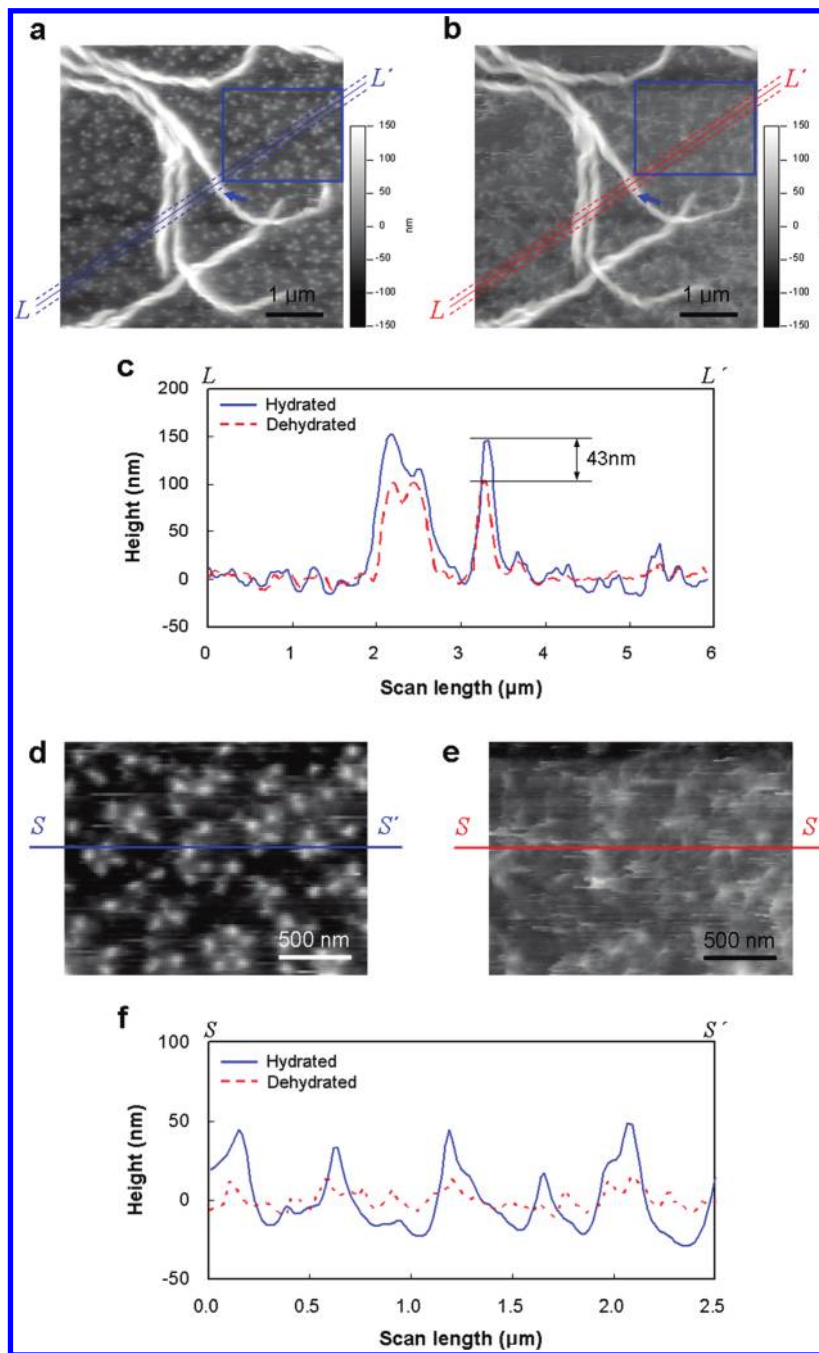


Figure 2. AFM topographical images of collagen fibrils at the same location (a) before and (b) after dehydration. The cross-section $L-L'$ is a representative section taken across the width of large fibrils. An overlay of cross-section data taken across the same large fibril shown in part c details a representative height change observed in large fibrils after dehydration. (d) Magnified image of the small bed of hydrated collagen fibrils from a region of part a enclosed by a box. (e) Magnified image of the small bed of dehydrated collagen fibrils from a region of part b enclosed by a box. (f) $S-S'$ is a representative section taken on the bed of small fibrils before and after dehydration.

Table 1. Comparison of AFM Topographies of Collagen Fibril Films Before and After Dehydration

	before dehydration	after dehydration
centerline average surface roughness with large fibrils, R_a (nm)	67 ± 13	47 ± 9^a
centerline average surface roughness of underlying bed of small fibrils, R_a (nm)	45 ± 12	30 ± 7^a
height of large fibrils (nm)	147 ± 18	118 ± 15^a
thickness of bed of small fibrils (nm)	410 ± 30	160 ± 10^a

^a Indicates a statistically significant difference after dehydration.

of about 250 and 70 nm for the fully hydrated and dehydrated layers, respectively, before a gradual increase in the apparent modulus as the stiffer glass substrate begins to dominate the

measurement. Large variability was observed for penetrations of less than 50 and 25 nm for fully hydrated and dehydrated fibrils, respectively, resulting from instrumental noise and uncertainties

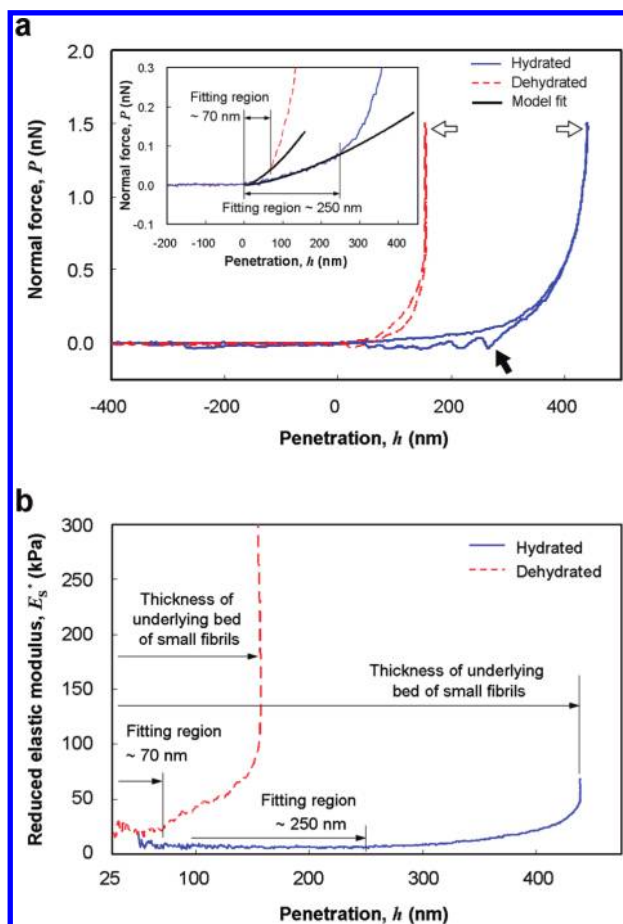


Figure 3. (a) Force–penetration curve and (b) the reduced elastic modulus of the bed of small fibrils before and after dehydration. A magnified region of the force–penetration curve is provided as an inset in part a. White arrows in part a indicate that the probe samples the substrate at larger forces, while a black arrow indicates that adhesion events are more significant for the bed of collagen fibrils before dehydration.

in determining the point of contact²¹ and these data were removed from the analysis. E_s^* values were determined within the penetration ranges indicated in Figure 3b and were 6.1 ± 0.8 kPa for fully hydrated films and significantly greater, 22 ± 4 kPa, after dehydration. The increase in modulus arising from the probe sensing the substrate allowed the thickness of the bed of hydrated small fibrils to be estimated as 410 ± 30 nm. Consistent with the topography measurements, the thickness of the bed of small fibrils was significantly smaller, 160 ± 10 nm, after dehydration. On the basis of the size and diameter of the small fibrils, the thickness of the compressed fibrillar layers between the probe and substrate at peak load were probably much smaller than the estimated thicknesses of the beds of small fibrils and hence had negligible effect on thickness estimation.

Observations of the small fibril bed such as those in Figures 1 and 2 indicate that the density of fibrils in the bed is inhomogeneous, with a structure including “clumps” of fibrils somewhat separated from each other, and not forming an interconnected gel. As a consequence, on loading the bed normal to the substrate the clumps will compress individually with little communication of strain to adjacent clumps of fibrils and thus generate little, but not zero, transverse strain in the overall small fibril foundation.

(21) Mahaffy, R. E.; Shih, C. K.; MacKintosh, F. C.; Kas, J. *Phys. Rev. Lett.* **2000**, *85*, 880–883.

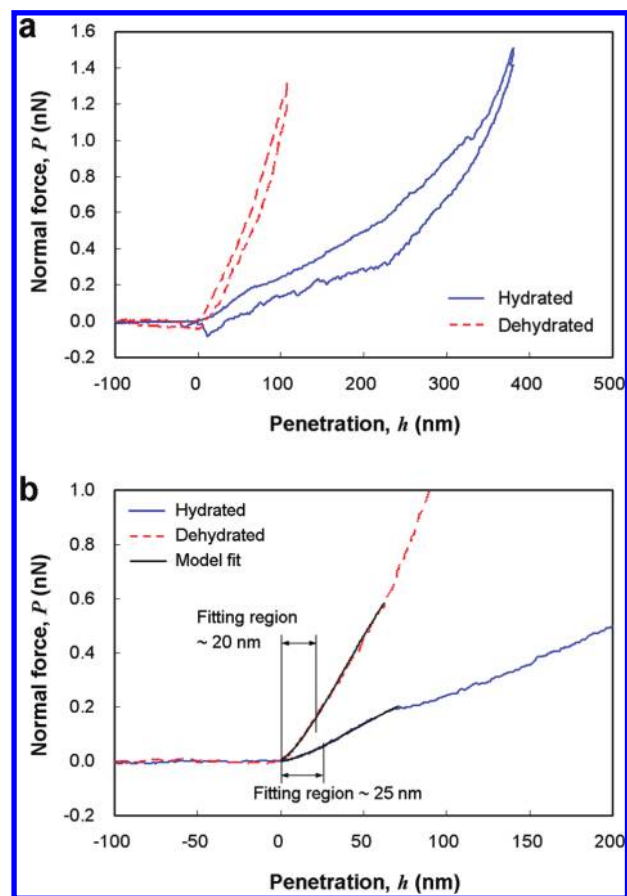


Figure 4. Representative force–penetration curves on a large fibril before and after dehydration obtained by gold-coated silicon nitride probe and shown at (a) full scale or (b) shown magnified with only the extension curve shown for clarity. The black solid lines appended to part b indicate the regions of data that were used in the calculation of elastic modulus values for large collagen fibrils.

The Poisson’s ratio of the bed of small fibrils is thus expected to be very small, certainly much less than the value of 0.5 appropriate for a fully interconnected gel, but not 0, as would be appropriate for a fully disconnected structure in the manner of a Winkler foundation.¹⁸ Here the value of the Poisson’s ratio of the bed of small fibrils was taken as $\nu_s = 0.1$, leading to negligible effects in deducing Young’s moduli from the measured indentation moduli of the bed. Consideration of eq 3 indicates that, for small values of ν_s , the assumed value of Poisson’s ratio also has a very small effect on the inferred foundation modulus of the bed of small fibrils.

Elastic Modulus of the Large Collagen Fibrils. Force–penetration measurements on the large fibrils were also performed, and together with the measurements on the underlying bed of smaller fibrils, were applied in a beam on elastic foundation model to determine the longitudinal elastic modulus, E_L , of the large fibrils. Representative force–penetration curves on the same fibril before and after dehydration are shown in Figure 4a. The curves in Figure 4 exhibit hysteresis, probably due to nonelastic effects such as poroelastic deformation of the porous fibrillar network in the aqueous solution. However, the highly reproducible force curves obtained at the same location and the comparison of AFM images before and after indentation (Supporting Information, Figure S3) suggest a largely elastic response of the large fibril on small fibril bed system. A schematic diagram of the elastic bending of a large collagen fibril on an elastically supporting

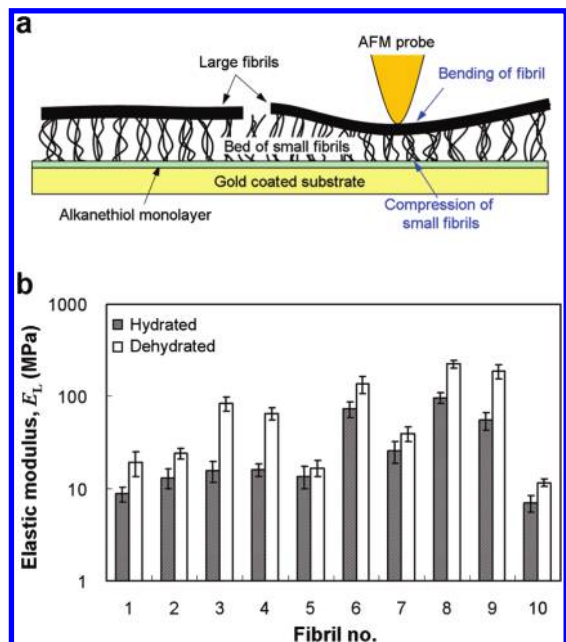


Figure 5. (a) Schematic diagram of the collagen thin film indented by the conventional AFM probe and (b) summarized data of the elastic modulus of the individual large fibrils. The error bars represent 1 standard deviation of the measured quantities.

bed of smaller fibrils under the AFM probe is shown in Figure 5a. Magnified regions of the force–penetration loading curves are shown in Figure 4b along with the fits from the model, eqs 2 and 3. The fitting region was the initial penetration to a depth less than 30% of the radius of the large fibrils, although the model fits the experimental data well to penetrations somewhat less than a large fibril radius. Applicability of the model can be further assessed by the fact that the inferred elastic moduli of the large fibrils yields a characteristic length scale for deformation, $(1/\lambda)$, that is much smaller than the fibril length, l , such that $\lambda l \gg 1$; $\lambda l \approx 11\text{--}17$ was observed here. Fully hydrated fibrils exhibit a wide range of longitudinal elastic moduli of 7 to 97 MPa. The same fibrils after dehydration also show a broad range, 12–230 MPa. The range of modulus values we observe for fully hydrated and dehydrated collagen fibrils could be the result of differences in the individual fibrils including: size,²² the rope like structure of the collagen fibrils,²³ or the orientation of collagen fibrils relative to the probe during indentation.^{22–25} In addition, the modulus measurements reported in this work might be influenced by the anisotropic nature of collagen fibrils, an effect reported for dried collagen fibrils indented in air at loading forces greater than 300 nN with an AFM tip.²⁴ Interestingly, this anisotropic effect is not observed in collagen fibrils indented under liquid at forces less than 4 nN with an AFM tip in a experimental setup similar to the one describe here.²⁵ A summary of the longitudinal elastic modulus calculated for the tested fibrils before and after dehydration is shown in Figure 5b (note the logarithmic scale). The mean modulus values for fully hydrated and dehydrated fibrils were significantly different, 32 and 81 MPa.

Prediction of the Effective Elastic Modulus of the Thin Film Structure. The stiffness of the overall composite structure

(22) Yang, L.; Van der Werf, K. O.; Fitie, C. F. C.; Bennink, M. L.; Dijkstra, P. J.; Feijen, J. *Biophys. J.* **2008**, *94*, 2204–2211.

(23) Bozec, L.; van der Heijden, G.; Horton, M. *Biophys. J.* **2007**, *92*, 70–75.

(24) Wenger, M. P. E.; Bozec, L.; Horton, M. A.; Mesquida, P. *Biophys. J.* **2007**, *93*, 1255–1263.

(25) Grant, C. A.; Brockwell, D. J.; Radford, S. E.; Thomson, N. H. *Appl. Phys. Lett.* **2008**, *92*, 233902.

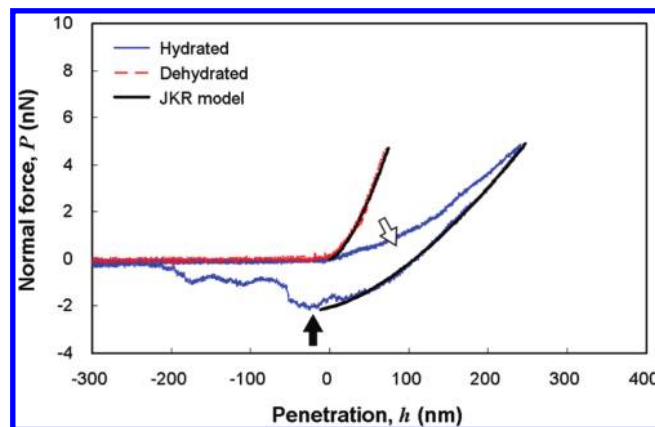


Figure 6. Force–penetration curves on the fully hydrated (blue solid line) and dehydrated (red dotted line) collagen thin films obtained from colloidal probe measurements at 5 nN normal force. Larger hysteresis (white arrow), as well as more significant and prolonged adhesion event (black arrow) is observed before dehydration. Black solid lines on the force–penetration curve illustrate data fitting to the JKR theory.

contains contributions from both the individual larger fibrils and the bed of smaller fibrils. A two-layer composite model can be used to estimate the effective elastic modulus of the entire film composed of both components by treating the components as lamina in parallel and a simple volume-fraction based rule of mixtures:

$$\frac{1}{E_T} = \frac{V_L}{E_L} + \frac{V_S}{E_S} \quad (4)$$

where E_T is the effective elastic modulus of the entire collagen thin film, and V_L and V_S are the volume fractions of the large and small fibril layers. The volume fraction of the larger fibrils for use in eq 4 was obtained from five AFM images of $20 \mu\text{m} \times 20 \mu\text{m}$ scans. The volume fraction of the smaller fibrils was estimated by multiplying the area fraction from the AFM image with the thickness determined from the force–penetration curves. The volume fractions of the large fibril and small fibril components were 0.24 and 0.76, respectively, before dehydration and 0.44 and 0.56 after dehydration. Using the average values of the elastic moduli of the 10 large fibrils (E_L) along with the average values of elastic moduli for the bed of small fibrils, the effective elastic moduli of the entire collagen thin film structure, E_T , before and after dehydration were estimated to be 8 ± 1 kPa and 40 ± 9 kPa, respectively.

Effective Measured Elastic Modulus of the Thin Film Structure. The mechanical properties of the thin film structure were measured using a colloidal probe attached to the AFM cantilever.²⁶ The larger probe size ($30 \mu\text{m}$ radius), compared to the unmodified AFM probe (20nm radius) was expected to sample the average mechanical properties of the composite collagen thin film structure composed of many larger individual fibrils together with the bed of smaller fibrils underneath them.

As observed in Figure 6, the force–penetration responses for the colloidal-probe measurements were hysteretic, indicative of large adhesive forces present between the colloidal probe and the collagen thin film, particularly in the hydrated state. The force–penetration responses were fit using the Johnson–Kendall–Roberts (JKR) model,²⁷ which takes adhesion into consideration in

(26) Dimitriadis, E. K.; Horkay, F.; Maresca, J.; Kachar, B.; Chadwick, R. S. *Biophys. J.* **2002**, *82*, 2798–2810.

(27) Johnson, K. L.; Kendall, K.; Roberts, A. D. *Proc. London R. Soc. A—Math. Phys. Eng. Sci.* **1971**, *324*, 301–313.

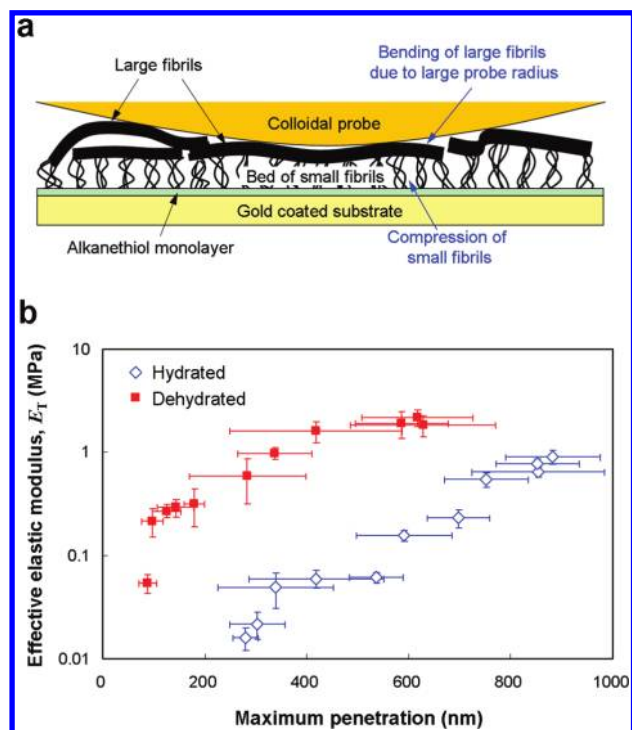


Figure 7. (a) Schematic diagram of the collagen thin film indented by the colloidal probe and (b) summarized data of the elastic modulus of the entire collagen sample with respect to penetration depth. The error bars represent one standard deviation of the measured quantities.

calculating the modulus of the film. Representative force–penetration curves on fully hydrated and dehydrated collagen thin films obtained with the colloidal probe under 5 nN normal peak forces, together with JKR model fits are shown in Figure 6. The JKR model fit the experimental force–penetration curves on both the fully hydrated and dehydrated samples (Figure 6) for 5 nN peak forces through the entire range. However, as the peak force was increased to 30 nN and beyond, discrepancies between experimental results and JKR model fits were apparent, suggesting a response from the stiff supporting glass substrate (data not shown).

A schematic diagram of the interaction between the colloidal probe and the collagen thin film is shown in Figure 7a. The effective elastic modulus of the entire collagen thin film, E_T (determined by assuming a Poisson's ratio of 0.2)^{28,29} with respect to the maximum penetration depth is summarized in Figure 7b. It was found that the effective elastic modulus of the fully hydrated thin film structure at approximately 300 nm penetration (about 5 nN force) was 16 ± 4 kPa. For approximately 80 nm penetration (same force), the modulus of the dehydrated thin film was significantly greater, 50 ± 10 kPa (*t*-test with equal variances). These values are similar to those estimated from the two-layer composite model. Although the stress field beneath the spherical probe is not exactly homogeneous as is assumed in the laminar composites estimation, the large probe used suggests that the majority of the film structure experienced simple compression during the colloidal probe measurements.

As the peak force was increased, the elastic moduli for both samples increased significantly and did not agree with the two-layer model estimate. For peak forces of approximately 150 nN,

corresponding to penetrations of approximately 850 and 600 nm for fully hydrated and dehydrated collagen thin films, respectively, the maximum penetration ceased increasing with increasing peak force suggesting that the probe had fully compressed the film between the underlying stiff gold coated glass substrate (Figure 7b and Figure S4 in Supporting Information). The maximum indentation depths for fully hydrated and dehydrated collagen thin films determined by using the colloidal probe were larger than the estimated thickness of the bed of small fibrils ($410 \text{ nm} \pm 30$ and $160 \text{ nm} \pm 10$ nm for fully hydrated and dehydrated collagen) and therefore, it was concluded that several large fibrils were indented by the colloidal probe.

Discussion and Summary

In this study we used quantitative AFM to evaluate fundamental mechanical properties of Type I collagen fibrils as a component of collagen films. Measurement of the mechanical properties of collagen fibrils in these thin films presents challenges not associated with classical mechanical measurements. Such challenges arise from the lateral and vertical structural heterogeneity of the films (Figure 1), the small dimensions of characteristic components of these films (< 200 nm), the small thickness of the films (≈ 600 nm), and the performance of these measurements in an aqueous buffer.

As depicted in Figure 1, these thin films are composed of a distribution of larger fibrils on a bed of small fibrils. To determine the modulus values for the larger fibrils within these films, we developed a new method of analysis based on a beam on an elastic foundation model described in the Supporting Information. This model incorporates data collected from the fibril topography observed from AFM imaging, AFM force–penetration curves on the bed of smaller fibrils, and AFM force–penetration curves on individual larger collagen fibrils. Through the use of this method we have determined that the bed of smaller fibrils has an elastic modulus of 6.2 ± 0.8 kPa and the larger fibrils have an average longitudinal modulus of 32 MPa. The values reported here for the moduli of individual 100–200 nm diameter collagen fibrillar components of a cell culture matrix are the first of which we are aware. The modulus of the entire film structure was estimated from a laminar composite model using these values as 8 ± 1 kPa. Large diameter colloidal probe AFM measurements were used to sample a large area of the film structure and provide information about the aggregate response. The elastic modulus of the fully hydrated collagen film measured with the colloidal probe was 16 ± 4 kPa, and compares favorably with the calculated composite value.

AFM was also used to characterize the collagen films after dehydration. Elastic modulus was observed to increase after dehydration, and topographical features were observed to decrease in scale. These observations are consistent with the likely role that water plays in the structure of collagen and the interaction of collagen fibrils.^{19,30–33} The mean elastic moduli increased to 81 MPa for the larger fibrils and 22 ± 4 kPa for the bed of smaller fibrils. The modulus of the composite collagen film was calculated to be 40 ± 9 kPa, which was in good agreement with the value experimentally determined using the colloidal probe of 50 ± 10 kPa, providing further validation of the beam on an elastic

(30) Mogilner, I. G.; Ruderman, G.; Grigera, J. R. *J. Mol. Graph.* **2002**, *21*, 209–213.

(31) Melacini, G.; Bonvin, A.; Goodman, M.; Boelens, R.; Kaptein, R. *J. Mol. Biol.* **2000**, *300*, 1041–1048.

(32) Kopp, J.; Bonnet, M.; Renou, J. P. *Matrix* **1990**, *9*, 443–450.

(33) Berisio, R.; Vitagliano, L.; Mazzarella, L.; Zagari, A. *Biopolymers* **2000**, *56*, 8–13.

(28) Barocas, V. H.; Moon, A. G.; Tranquillo, R. T. *J. Biomech. Eng.—Trans. ASME* **1995**, *117*, 161–170.

(29) Parekh, A.; Velegol, D. *Ann. Biomed. Eng.* **2007**, *35*, 1231–1246.

foundation model. The finding that dehydration results in an increase in modulus of the collagen film is consistent with our previous observations that dehydrated collagen films provide signals to cells that result in increased spreading and proliferation, and other observations that are consistent with cell response to stiffer matrices.⁶

We observed a difference of several orders of magnitude in the elastic modulus of the individual larger fibrils and the underlying bed of smaller fibrils. Previous studies have been reported on the compression,²⁵ and pulling³⁴ of isolated fibrils with diameters of 200 to 500 nm and adsorbed onto solid surfaces. These measurements were made in buffer and resulted in values of ≈ 1 and ≈ 30 MPa, respectively. These values compare to mean elastic moduli of 32 and 81 MPa that we report here for fully hydrated and dehydrated fibrils. That large fibrils have such a large elastic modulus is a surprising finding, given the observed movement of large fibrils by cells,⁶ which suggests that cells sense and manipulate the large fibrils. We have observed that the ability of cells to manipulate large fibrils is highly dependent on whether collagen films are fully hydrated or dehydrated, and the failure of cells to move the larger fibrils is associated with cell spreading, proliferation, and other characteristics of cells in a contractile phenotype. Such data suggest that the mechanics of movement of the larger collagen fibrils is highly relevant to cell response. While the current study has examined collagen fibrils by measuring forces applied normal to the collagen film, it is possible that lateral stiffness, which was not measured in this study, is also likely to be very important in cell sensing of the ECM. Semiquantitative observations of lateral displacement of a mass of larger fibrils of a collagen film using an AFM tip indicated that fully hydrated fibrils can be laterally displaced by applying a force of 5 nN at the AFM tip; after dehydration, the application of 100 nN of force was insufficient to alter the location of the larger collagen fibrils³⁵ (see also Supporting Information Figure S5). While quantification of lateral forces associated with collagen fibrils is a great challenge, such a study is ongoing.

The results of this study also suggest that topography may play an important role in cell response to collagen, given the difference in topography that was measured as a result of dehydration of collagen films. Recent micropatterning experiments³⁶ provide new insight into how topography might influence rates of migra-

tion of cells as a result of affects on cell spreading. An important issue that the use of thin films for cell culture raises is that cells may actually sense the substrate that the collagen thin film is grown on.³⁷ We have experimentally determined in a separate publication⁷ that cells on these thin collagen fibril films (≈ 400 – 600 nm) behave similarly to millimeter thick collagen gels in terms of morphology, actin stress fibril formation, and ECM production. In addition, we have published a recent study³⁸ that directly compares cell response on films with a thin coating of nonfibrillar collagen and on the thicker hydrated collagen fibrils. From these previous results based on data collected for several cell responses we believe the influence of the underlying substrate below the hydrated collagen fibril films on cell behavior is minimal. As added proof, our findings are in line with a recent publication³⁷ that illustrates cell spreading is inhibited on compliant films with thickness of 500 nm or 70 μm that have modulus values similar to those we report.

The composite values observed in our experiments for fully hydrated collagen films are similar to modulus measurements reported for *in vivo* tissues, such as breast tissue (≈ 1 kPa)³⁹ and skin (≈ 10 kPa).⁴⁰ Our reported values of around 40 kPa for the collagen films are also on the order of the modulus to which muscle cells are reported to respond in studies that use polyacrylamide to modify the compliance of the cell substrate. The films of collagen that are the focus of this study allow an unprecedented examination of the topographical and mechanical characteristics of a bed of collagen fibrils, adding to our knowledge of how nanoscale features of matrix can influence cell response.

Acknowledgment. The authors would like to thank Dr Gregory Vogl of NIST and Dr Michelle Oyen of Cambridge University for helpful discussions regarding the nonlinear equation describing a cylindrical beam on an elastic foundation. We also acknowledge the helpful discussions with Dr. Gordon A. Shaw from NIST.

Supporting Information Available: Supplementary figures and text giving details for mechanics of a cylindrical beam on an elastic foundation. This material is available free of charge via the Internet at <http://pubs.acs.org>.

(37) Sen, S.; Engler, A. J.; Discher, D. E. *Cell. Mol. Bioeng.* **2009**, *2*, 39–48.

(38) Bhadriraju, K.; Chung, K.-H.; Spurlin, T. A.; Haynes, R. J.; Elliott, J. T.; Plant, A. L. *Biomaterials* **2009**, *30*, 6687–6694.

(39) Paszek, M. J.; Zahir, N.; Johnson, K. R.; Lakins, J. N.; Rozenberg, G. I.; Gefen, A.; Reinhart-King, C. A.; Margulies, S. S.; Dembo, M.; Boettiger, D.; Hammer, D. A.; Weaver, V. M. *Cancer Cell* **2005**, *8*, 241–254.

(40) Tilleman, T. R.; Tilleman, M. M.; Neumann, M. H. *Isr. Med. Assoc. J.* **2004**, *6*, 753–755.

(34) Graham, J. S.; Vomund, A. N.; Phillips, C. L.; Grandbois, M. *Exp. Cell Res.* **2004**, *299*, 335–342.

(35) Spurlin, T. A.; Bhadriraju, K.; Chung, K.-H.; Tona, A.; Plant, A. L. *Biomaterials* **2009**, *30*, 5486–5496.

(36) Petrie, R. J.; Doyle, A. D.; Yamada, K. M. *Nat. Rev. Mol. Cell Biol.* **2009**, *10*, 538–549.